Journal of Engineering Physics and Thermophysics, Vol. 79, No. 3, 2006

TWO-DIMENSIONAL MODEL OF HEAT AND MASS TRANSFER IN THE PROCESS OF FRACTIONAL CRYSTALLIZATION ON A BAND

P. P. Osipov

UDC 66.065.52:548.5

A two-dimensional model of heat and mass transfer in the process of fractional crystallization on a band is proposed. Algorithms for calculating the concentration of an impurity in a melt have been developed and the impurity distributions in a diffusion layer have been obtained for the cases of linear-profile and wavy-profile crystals on the basis of numerical experiments. It has been established that the impurity distribution is two-dimensional in the case of a wavy-profile crystal.

Introduction. The distribution of an impurity near a growing crystal was investigated with the use of one-dimensional models in [1–7]. In the present work, we investigated the fractional crystallization in a band crystallizer (Fig. 1). This crystallization is a new process proposed by researchers of the University of Bremen for fine purification of substances [8–10].

A melt is fed on the upper part of a cooled inclined band. Then the melt runs down by the band to a lower tank, from which it is fed again into the circulation loop. In zones 1, 2, and 3, the lower part of the band is sprayed by water at three different temperatures. As a result of the cooling of the band, a thin crystal layer is formed in zone 3 of its surface. This crystal moves up together with the band surface, and its thickness increases with decrease in the cooling temperature in the direction from zone 3 to zone 1. The crystal formed is removed by a scraper installed on an upper drum. The above-described process of crystal formation as a whole is steady-state and continuous, which substantially differentiates it from the analogous known processes. It should be noted that, in this case, the purity of the crystal can be many times higher than the purity of the melt.

A model of one-dimensional heat and mass transfer in the process of crystallization on a band has been proposed in [11]. This model made it possible to optimize the fractional crystallization on a band and propose a forward-flow scheme for it [12, 13]. One-dimensional models are simple and convenient; however, the boundaries of their use are not always known. In the present work, a two-dimensional model of mass transfer is proposed. This model allows one to calculate the concentration of an impurity in a melt more exactly and to determine the boundaries of applicability of one-dimensional models.

Two-Dimensional Model of Heat Transfer. We will consider a stationary-profile crystal on a cooled moving band. The thickness of the crystal $\delta_c(x)$ is somewhat distributed along the length of the band (Fig. 2). In this case, any two-dimensional temperature distributions are established in the crystal and in the band (the temperature diagram in Fig. 2 is denoted by the dotted line).

The following main assumptions will be used: 1) the temperature on the surface of the crystal is equal to its melting point T_m calculated by the diagram of phase states at an impurity concentration c_0 [6]; 2) the densities of the crystal and the melt are equal.

Rate of Crystallization. The rates of crystallization at different points of the crystal surface are, by and large, different. The local rate of crystallization is determined from the ratio $V_c(x) = -u_b \dfrac{d\delta_c/dx}{\sqrt{1 + (d\delta_c/dx)^2}}$. In practice, a crystal layer is fairly thin and its thickness increases gradually from 0 to 3–7 mm along a length of ~3 m. Therefore, the derivative $d\delta_c/dx$ is of the order of 0.01–0.001 and the local rate of crystal growth is equal to

Institute of Mechanics and Machine Building, Kazan' Scientific Center, Russian Academy of Sciences, 2/31 Lobachevskii Str., Kazan', 420111, Russia; email: petro300@rambler.ru. Translated from Inzhenerno-Fizicheskii Zhurnal, Vol. 79, No. 3, pp. 30–36, May–June, 2006. Original article submitted November 1, 2004; revision submitted March 22, 2005.

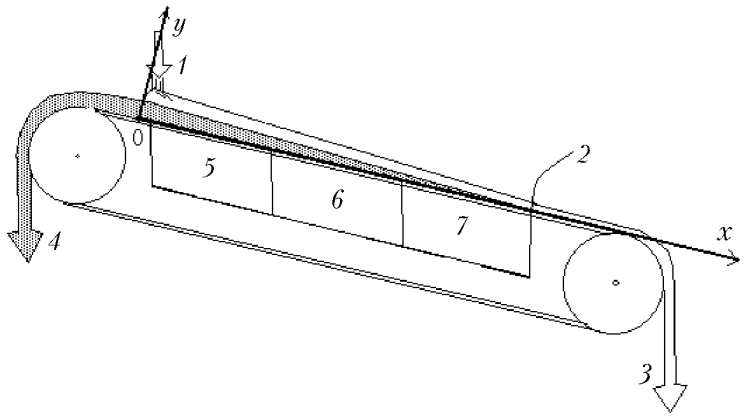

Fig. 1. Diagram of a band for continuous fractional crystallization: 1) power source; 2) beginning of crystallization; 3) melt; 4) crystal; 5) cooling zone 1; 6) zone 2; 7) zone 3.

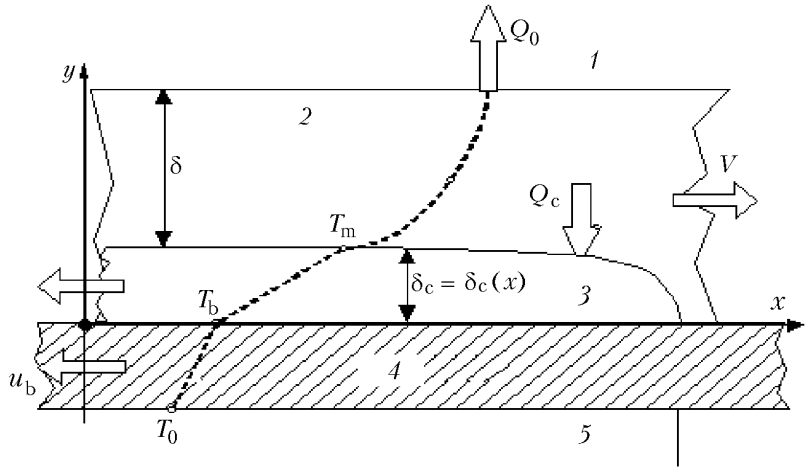

Fig. 2. Scheme of heat transfer in the process of crystallization on the band: 1) evaporation and convection; 2) melt film; 3) crystal; 4) band; 5) cooling zone 3.

$$V_c(x) = -u_b \frac{d\delta_c}{dx}. \tag{1}$$

Heat Transfer in the Band–Crystal–Film System. Below are presented the main computational regions, as well as equations and boundary conditions for the heat transfer in a film of a melt, in a band, and in a crystal.

Melt film. The heat balance for the melt flowing in the region $0 \le x \le l$ can be defined as

$$\delta R \rho V \frac{dT}{dx} = -\alpha \left\{ T(x) - T_m \right\} - Q_0. \tag{2}$$

Introducing the characteristic thickness of the melt film $\Delta = \left(\frac{3\nu^2}{g \sin\beta} \right)^{1/3}$, we will write the known relations for the film thickness in the following form: $\delta/\Delta = 0.302\ \mathrm{Re}^{8/15}$ for $\mathrm{Re} \ge 400$ and $\delta/\Delta = \mathrm{Re}^{1/3}$ for $\mathrm{Re} < 400$ [14, 15]. The authors of these works also propose empirical formulas for determining the heat-transfer coefficient $\alpha = \frac{\mathrm{Nu}}{\delta}\lambda$:

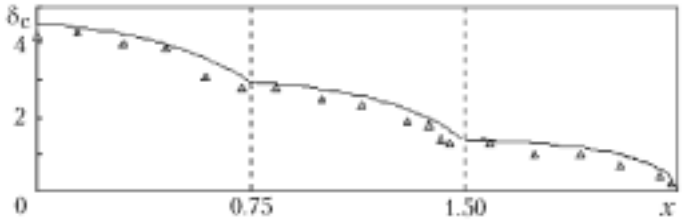

Fig. 3. Profile of a crystal for l = 2.25 m: points are experimental data of the author; curves are calculation data obtained with the use of a one-dimensional model of heat transfer [11]. δ_c, mm.

$$\mathrm{Nu} = 1.88\,, \quad \mathrm{Re} < \mathrm{Re}^* = 615\mathrm{Pr}^{-0.646}\,; \quad \mathrm{Nu} = 0.0614\mathrm{Re}^{8/15}\mathrm{Pr}^{0.344}\,, \quad \mathrm{Re}^* < \mathrm{Re} < 400\,;$$

$$\mathrm{Nu} = 0.00112\mathrm{Re}^{6/5}\mathrm{Pr}^{0.344}\,, \quad 400 < \mathrm{Re} < 800\,; \quad \mathrm{Nu} = 0.0066\mathrm{Re}^{14/15}\mathrm{Pr}^{0.344}\,, \quad 800 < \mathrm{Re}\,.$$

The heat losses by the convection and evaporation Q_0 were determined by the author of the present work experimentally by the temperature of the melt at the end point of the band.

Band. In the region $0 \le x \le l$, $-\delta_b \le y \le 0$

$$-u_b \frac{\partial T_b}{\partial x} = a_b \left(\frac{\partial^2 T_b}{\partial x^2} + \frac{\partial^2 T_b}{\partial y^2} \right), \tag{3}$$

on the cooled side of the band, the temperature is equal to

$$T_b\,(x, -\delta_b) = T_0\,(x)\,, \tag{4}$$

and, at the band–crystal interface, the temperature distribution and the heat flow are continuous, i.e.,

$$T_b\,(x, 0) = T_c\,(x, 0) \quad \text{and} \quad \lambda_b \frac{\partial T_b}{\partial y}\,(x, 0) = \lambda_c \frac{\partial T_c}{\partial y}\,(x, 0)\,. \tag{5}$$

Note that in the case where there are three cooling zones, $T_0(x)$ is a piecewise function.

Crystal. In the region $0 \le x \le l$, $0 \le y \le \delta_c(x)$

$$-u_b \frac{\partial T_c}{\partial x} = a_c \left(\frac{\partial^2 T_c}{\partial x^2} + \frac{\partial^2 T_c}{\partial y^2} \right), \tag{6}$$

on the melt side, the temperature is equal to the crystallization temperature

$$T_c\,(x, \delta_c\,(x)) = T_m\,, \tag{7}$$

the local rate of crystallization is related to the average temperature of the melt $T(x)$ by the relation

$$V_c\,(x) = -u_b \frac{d\delta_c\,(x)}{dx} = \frac{Q_c\,(x) - \alpha\left\{T\,(x) - T_m\right\}}{\rho_c H}\,, \tag{8}$$

where $Q_c(x) = \lambda_c \dfrac{\partial T_c}{\partial y}\,(x,\ \delta_c(x))$ is the heat flow at the crystal boundary.

Crystal profile. In the general case, relation (8) determines the thickness of a crystal along the band. If the band moves with a low velocity (<1 mm/sec), the longitudinal heat conduction and convection in the band and in the

crystal can be disregarded. In this case, the formula for the one-dimensional (transverse) heat transfer $Q_c(x) = [T_m - T_0(x)]/\left(\frac{\delta_c(x)}{\lambda_c} + \frac{\delta_b}{\lambda_b}\right)$ can be used, and the crystal profile is determined by the ordinary differential equation

$$\rho_c H u_b \frac{d\delta_c(x)}{dx} = \mathrm{Nu}\,\lambda \frac{T(x) - T_m}{\delta} - \frac{T_m - T_0(x)}{\frac{\delta_c(x)}{\lambda_c} + \frac{\delta_b}{\lambda_b}}.$$

Figure 3 shows a wavy crystal profile typical for the zonal cooling.

Two-Dimensional Model of Mass Transfer. We will consider the mass transfer in the melt layer near the surface of a crystal. The concentration of an impurity in this layer is conveniently determined with the use of a curvilinear orthogonal coordinate system. In this system, the coordinate lines x = const coincide with the normals to the surface of the crystal and the line $y = 0$ coincides with this surface. The quantity y characterizes the distance to the crystal surface.

Similarity between Heat Transfer and Diffusion. The heat flow from a melt film to a crystal can be defined as $q = \alpha[T(x) - T_m]$. On the other hand, this flow can be expressed in terms of the characteristic size δ_h as $q = \frac{\lambda}{\delta_h}[T(x) - T_m]$. Comparison of these expressions shows that $\delta_h = \delta/\mathrm{Nu}$. This quantity determines the thickness of the layer in which the main heat transfer proceeds. At large Reynolds numbers, this thickness is equal to the thickness of the boundary layer. In the present investigation, the value of $\delta_h \approx 10^{-3}$ m is used. It is known that, in the process of crystal growth, an impurity is forced out to the melt; because of this, the impurity concentration near the crystal surface is higher than the impurity concentration in the main mass of the melt. This excess impurity is carried out from the diffusion layer as a result of the diffusion, is picked up by the high-velocity part of the melt flow, and is carried along the band. An impurity-concentration gradient gives rise to a mass transfer in the diffusion layer. The dimensionless concentration gradient is called the Sherwood number. The thickness of the diffusion layer, in which the main mass transfer proceeds, is determined on the basis of the known similarity between the heat transfer and the mass transfers, according to which:

$$\delta_d = \delta_h \left(\frac{\mathrm{Nu}}{\mathrm{Sh}}\right) = \delta_h \left(\frac{\mathrm{Pr}}{\mathrm{Sc}}\right)^{0.344} = \delta_h \left(\frac{D}{a} m^*\right)^{0.344}. \quad (9)$$

Since, for a typical crystallization, $a \cong 10^{-7}$ m^2/sec, $D \cong 10^{-10}$ m^2/sec, and $m^* \cong 1$ in the last-mentioned formula, the thickness of the diffusion layer is several tens of times smaller than the thickness of the layer in which the main heat transfer proceeds and is of the order of 10^{-4} m.

Velocity Distribution in the Diffusion Layer. Since the thickness of the diffusion layer is several tens of times smaller than the thickness of the heat-transfer layer, it may be suggested that the distribution of the velocity field along y is practically linear within this layer, i.e.,

$$V_x(y) = \frac{\tau_0}{\mu} y, \quad (10)$$

where $\tau_0 = \rho g \delta \sin \beta$ is the shear friction stress compensating the projection of the weight of the melt film on the flow direction x. A method for more exact estimation of the velocity profile is described in [16].

Convection and Diffusion of an Impurity. The concentration of an impurity in the diffusion layer $0 < x < l$, $0 < y < \delta_d$ is determined in the first approximation from the equation

$$V_x(y) \frac{\partial c}{\partial x} - V_c(x) \frac{\partial c}{\partial y} = D \left\{\frac{\partial^2 c}{\partial x^2} + \frac{\partial^2 c}{\partial y^2}\right\}. \quad (11)$$

It is assumed that, in Eq. (11), the velocity of the melt flow along y is equal in value to the local rate of crystal growth and is in opposition to it.

Boundary conditions. It may be assumed that, beyond the diffusion layer, the impurity is distributed homogeneously along the y coordinate. Moreover, since, in the case of fractional crystallization, the mass rate of a melt is usually much higher than the mass rate of a crystal, it may be suggested that the impurity concentration beyond the diffusion layer is practically constant and is equal to that in the feeding melt. Therefore, it is natural to assume that, at the diffusion-layer boundary $y = \delta_d$,

$$c\,(x, \delta_d) = c_0\,. \tag{12}$$

The following boundary condition can be set at the crystal–melt interface ($y = 0$) [1, 6]:

$$(k_0 - 1)\,V_c\,(x)\,c = D\,\frac{\partial c}{\partial y}\,. \tag{13}$$

The boundary condition at the point of melt feed $x = 0$ has the form

$$c\,(0, y) = c_0\,. \tag{14}$$

Diffusion-Layer Approximation. Let us introduce the dimensionless spatial coordinates $x^* = x/l$, $y^* = y/\delta_d$ and the concentration $c^* = c/c_0$. Omitting the asterisk and using the linear approximation (10) of the longitudinal velocity of the melt, we obtain, from (11), the following equation:

$$\frac{1}{\mathrm{Pe}\,(x)}\,y\,\frac{l_x}{l}\,\frac{\partial c}{\partial x} - \frac{\partial c}{\partial y} = \frac{1}{\mathrm{Pe}\,(x)}\left\{\left(\frac{\delta_d}{l}\right)^2\frac{\partial^2 c}{\partial x^2} + \frac{\partial^2 c}{\partial y^2}\right\}, \tag{15}$$

where $\mathrm{Pe}(x) = V_c(x)\delta_d/D$ is the Peclet number;

$$\frac{l_x}{\Delta} = 3\,\frac{\nu}{D}\left(\frac{\delta_c}{\delta}\right)^3\left(\frac{\delta}{\Delta}\right)^4 \cong 3\,\frac{\nu}{a}\,\frac{1}{\mathrm{Nu}^3}\left(\frac{\delta}{\Delta}\right)^4 \tag{16}$$

is the dimensionless characteristic length. The coefficient of $\partial^2 c/dx^2$ in (15) is always much smaller than unity. For example, for typical values of $\delta_d \cong 10^{-4}$ m and $l \cong 3$ m, we will obtain $(\delta_d/l)^2 \cong 10^{-9}$. This means that the diffusion along the melt flow can be disregarded and it is appropriate to use, instead of (15), the following equation:

$$\frac{1}{\mathrm{Pe}\,(x)}\,y\,\frac{l_x}{l}\,\frac{\partial c}{\partial x} - \frac{\partial c}{\partial y} = \frac{1}{\mathrm{Pe}\,(x)}\,\frac{\partial^2 c}{\partial y^2}\,. \tag{17}$$

The boundary conditions (12)–(14) can be rewritten in the dimensionless form

$$c\,(x, 1) = 1\,,\quad (k_0 - 1)\,c\,(x, 0) = \frac{1}{\mathrm{Pe}\,(x)}\,\frac{\partial c}{\partial y}\,(x, 0)\,,\quad c\,(0, y) = 1\,. \tag{18}$$

Results of Simulation. On the basis of the mass-transfer model, we numerically investigated the concentration distribution of an impurity in a diffusion layer.

Numerical Scheme. Problem (17), (18) is analogous from the mathematical standpoint to the problem on membrane purification and is solved by the finite-difference method [17]. A four-node (T-like) pattern with three nodal values of the next layer, expressed in terms of the previous central one, is used. In each layer x, the concentration distribution transverse to the diffusion layer is calculated by an implicit scheme. Below are results of simulation performed for a linear-profile and wavy-profile crystals.

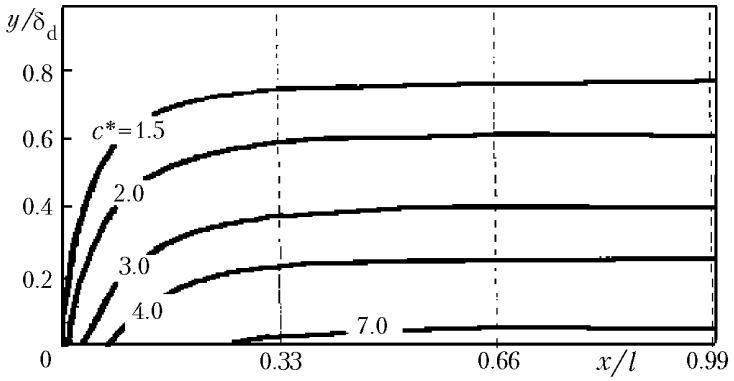

Fig. 4. Concentration of an impurity in a melt in the case of a linear-profile crystal for k_0 = 0.02, δ_d = 0.08 mm, and $V_c = 0.25 \cdot 10^{-5}$ m/sec.

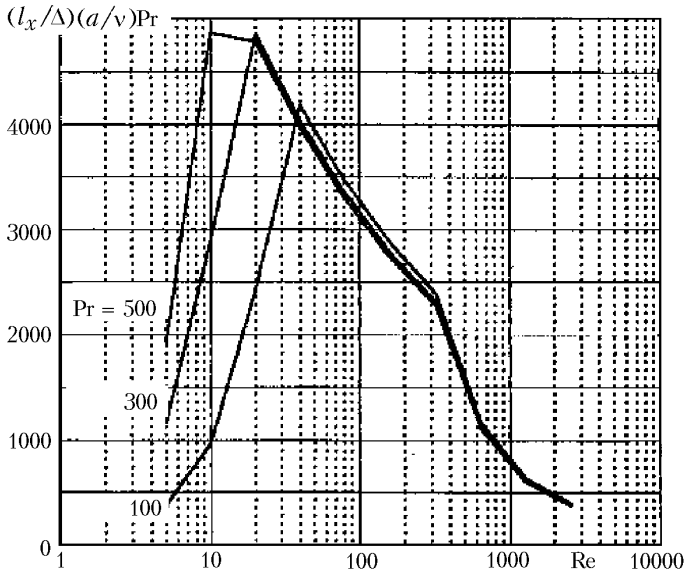

Fig. 5. Dependence of the transient-zone dimension on Re.

Constant Rate of Crystal Growth. A linear profile of a crystal is considered as optimum. According to (1), the rate of growth of a linear-profile crystal remains unchanged along the band. Because of this, the second boundary condition (18) does not lead to the appearance of a longitudinal concentration gradient, and the single reason for its appearance is the transient process near the point of melt feed. It is known [6] that many organic and inorganic systems are well purified when the rate of crystal growth does not exceed $V_c(x) \cong 0.25 \cdot 10^{-5}$ m/sec. Therefore, calculations were performed for these values. Numerical investigations have shown that there exists a transient region in which the concentration distribution of an impurity is two-dimensional. Figure 4 shows dimensional constant-concentration lines of an impurity in a melt. The length of the indicated region is equal to the characteristic length l_x, determined by relation (16). Beyond the transient region the diffusion process is practically one-dimensional.

Figure 5 presents the dependence of the dimension of the transient region (16) on the Reynolds number. For example, $\Delta \cong 0.6$ mm for $\nu = 2 \cdot 10^{-5}$ m^2/sec and $\beta = 40^o$. For Re = 20 and ν/a = 34, l_x = 0.51 m at Pr = 100 and l_x = 0.33 m at Pr = 300.

Variable Rate of Crystal Growth. It is difficult, from the technological standpoint, to obtain the linear-profile crystal considered above because, in this case, the intensity of cooling of a band should be continuously changed. It is much simpler to realize a sectionally continuous cooling (Fig. 1). In the case of such a cooling, a wavy-profile crystal is obtained at $u_b < 1$ mm/sec (Fig. 3). Because of the nonlinearity of the crystal profile, the rate of crystal growth can vary significantly along the length of the band (by three to eight times). In this case, the second boundary condi-

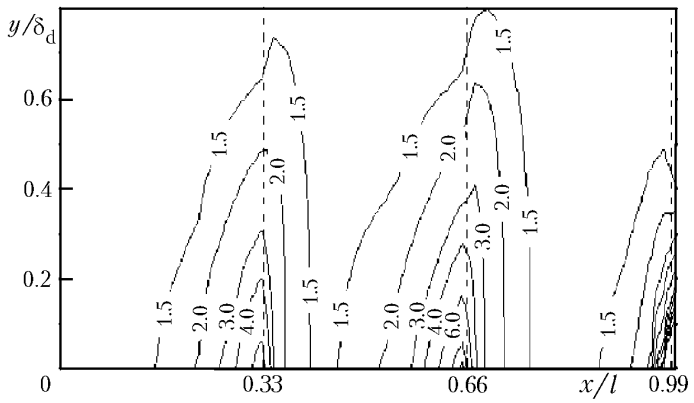

Fig. 6. Concentration of an impurity in a melt in the case of a wavy-profile crystal for $k_0 = 0.02$ and $\delta_d = 0.08$ mm. The values of the impurity concentration are dimensionless.

tion (18) leads to the appearance of large longitudinal concentration gradients, with the result that the concentration fields become not one-dimensional. The dimensionless constant-concentration lines of an impurity in a melt, presented in Fig. 6, are evidence in favor of the two-dimensional mass transfer.

Conclusions. The results of our numerical investigation of the concentration distribution of an impurity near a crystal formed on a band indicate that this distribution is mainly determined by the shape of the crystal. The impurity distribution is practically one-dimensional for a linear-profile crystal. This distribution is two-dimensional only in the transient region. The formula proposed in the present work for estimating the dimension of the transient zone allows one to determine the boundaries of applicability of the one-dimensional approach. In the case of a wavy-profile crystal, the concentration field of the impurity is two-dimensional everywhere.

NOTATION

$a = \lambda/R\rho$, thermal diffusivity; c_0 and c, initial and current concentrations of an impurity in a melt; $c^* = c/c_0$, dimensionless concentration of the impurity; D, diffusion coefficient; g, free fall acceleration; H, latent heat of crystallization; k_0, imaginary coefficient of impurity distribution; l, total length of the crystallization zones; l_x, length of the transient zone; m^*, ratio between the molar masses of the impurity and the melt; $\mathrm{Nu} = \alpha(\delta/\lambda)$, Nusselt number; Pe, Peclet number; $\mathrm{Pr} = \nu\rho R/\lambda$, Prandtl number; Q_0, heat-loss power density on the free surface of the melt; $Q_c(x)$, heat outflow at the crystal–band interface; $\mathrm{Re} = V\delta/\nu$, Reynolds number; R, specific heat capacity; $\mathrm{Sc} = m^*\nu\rho/D$, Schmidt number; Sh, Sherwood number; T_m, temperature of melting (crystallization) of the melt; $T(x)$, average temperature in the cross section of a melt film; $T_0(x)$, temperature of the cooled surface of the band; T_b and T_c, temperature of the band and the crystal; u_b, velocity of the band; V, velocity of the melt film averaged over its thickness; $V_x(y)$, transverse distribution of the longitudinal velocity component of the melt film; $V_c(x)$, rate of crystal growth; x and y, longitudinal and transverse coordinates of the crystal; α, coefficient of heat transfer between the crystal and the melt; β, angle of inclination of the band; δ_b, δ, and $\delta_c(x)$, thickness of the band, the melt, and the crystal; δ_h and δ_d, thickness of the heat-transfer and diffusion layers; Δ, characteristic thickness of a melt film; λ, heat-conductivity coefficient; μ and ν, dynamic and kinematic viscosities; ρ, density. Subscripts: b, band; d, diffusion; c, crystal; m, melting; h, heat transfer.

REFERENCES

1. J. Burton, R. Prim, and W. Slichter, The distribution of solute in crystals grown from the melt, *J. Chem. Phys.*, **21**, 1987–1991 (1953).
2. D. Hurle, Constitutional supercooling during crystal growth from stirred melts, *Solid-State Electronics*, **3**, No. 1, 37–44 (1961).
3. W. A. Tiller, Alloy crystal growth, in: *Proc. 3rd Int. Conf. on Crystal Growth*, New York (1958), pp. 332–341.

4. K. Wintermantel and W. Kast, Waerme und Stoffaustausch bei der Kristallisation an gekuehlten Flaechen, *Chem.-Ing.-Tech.*, **45**, No. 10, 728–731 (1973).

5. K. Wintermantel, Die effektive Trennwirkung beim Ausfrieren von Kristallschichten aus Schmelzen und Loesungen — eine einheitliche Darstellung, *Chem.-Ing.-Tech.*, **58**, No. 6, 498–499 (1986).
6. S. Myasnikov, B. Kazimbekov, V. Malyusov, and N. Zhavoronkov, Theoretical principles of fractional crystallization, *Teor. Osnovy Khim. Tekhnol.*, **18**, NO. 6, 749–760 (1984).
7. N. Lapin, D. Nikolaev, V. Malyusov, and N. Zhavoronkov, Capture of the melt during crystallization of organic systems forming the eutectics, *Teor. Osnovy Khim. Tekhnol.*, **10**, No. 1, 31–39 (1976).
8. I. Huenken, J. Ulrich, O. Fischer, and A. Koenig, Continuous and countercurrent layer crystallization, in: *Proc. 12th Symp. on Industrial Crystallization*, Vol. 1 (1993), pp. 148–158.
9. J. Ulrich, I. Huenken, O. Fischer, und A. Koenig, Eine Apparatur zur kontinuerlichen Stofftrennung mittels gerichteter Kristallisation, *GVC-Jahrestreffen der Verfahrensingenieure*, 30 Sept.–2 Oct. 1992, Wien, Austria (1992), **9**, pp. 242–244.
10. I. Huenken, Oezoguz, and J. Ulrich, A new apparatus for a continuous directed crystallization process, in: *Proc. BIWIC*, Verlag Mainz GmbH, Bremen, Germany (1991), pp. 112–122.
11. P. Ossipov, Continuous fractional crystallization on a moving cooled belt, *Int. J. Heat Mass Transfer*, **41**, No. 4–5, 691–697 (1998).
12. P. Ossipov, Optimization of heat-mass transfer at continuous solid layer crystallization on belt, *Appl. Math. Model.*, **23**, No. 5, 419–436 (1999).
13. P. Ossipov, Theoretical and experimental investigations of countercurrent and cocurrent schemes of fractional crystallization on a band, in: *Proc. 14th Int. Symp. on Industrial Crystallization*, UK, Cambridge, 12–16 September (1999), pp. 149–157.
14. H. Brauer, Stroemung und Waermeuebergang bei Rieselfilmen, *VDI Forschungsheft*, No. 457, 22–30 (1956).
15. W. Wilke, Waermeuebergang an Rieselfilme, *VDI Forschungsheft*, No. 490, 28–37 (1962).
16. N. Kulov, M. Murav'ev, V. Malyusov, and N. Zhavoronkov, Velocity profiles of a falling liquid film, *Teor. Osnovy Khim. Tekhnol.*, **16**, No. 4, 499–506 (1982).
17. R. Singh and R. Laurence, Influence of slip velocity at a membrane surface on ultrafiltration performance, *Int. J. Heat Mass Transfer*, **22**, No. 2, 721–729 (1979).